UNIVERSIDAD DISTRITAL
FRANCISCO JOSÉ DE CALDAS

Ingeniería

https://revistas.udistrital.edu.co/index.php/reving/issue/view/1291

DOI: https://doi.org/10.14483/23448393.23474

Research

Energy Management System using Particle Swarm Optimization for Operating Costs Reduction in AC Microgrids with Battery Storage during Grid-Connected and Islanded Operation

Sistema de gestión de energía mediante optimización por enjambre de partículas para la reducción de costos operativos en microrredes de CA con almacenamiento en baterías durante la operación interconectada y aislada

Hugo Alessandro Figueroa-Saavedra, Luis Fernando Grisales Noreña*, and Brandon Cortés Caicedo

[1]Department of Electrical Engineering, Faculty of Engineering, Universidad de Talca, Curicó 3340000, Chile
[2]Grupo de Investigación en Alta Tensión-GRALTA, Escuela de Ingeniería Eléctrica y Electrónica, Universidad del Valle, Cali 760015, Colombia
[3]Department of Engineering, Institución Universitaria Pascual Bravo, Robledo campus, Medellín 050036, Colombia

Abstract

Context: This paper proposes an energy management system (EMS) for battery energy storage systems (BESS) to reduce operating costs in AC microgrids (MGs) operating in grid-connected (GON) and islanded (GOFF) mode, considering energy purchase, conventional generation, and maintenance costs while accounting for all the operational constraints of the system and its components.
Method: A master-slave methodology based on particle swarm optimization (PSO) and an hourly power flow based on the successive approximations method (SAM) is used as a smart BESS operation strategy. This proposal is validated in a 33-bus AC-MG operating in GON and GOFF modes, in comparison with two methods utilizing the vortex search algorithm (VSA) and conitnuos version of the Chu & Beasley genetic algorithm (CBGA) and the same power flow.
Results: The PSO-based EMS achieved the lowest costs *i.e.*, 6897.59 USD/day (GON) and 17 527.42 USD/day (GOFF), with cost reductions of 1.45 and 0.13 %, and low standard deviation values (0.067 and 0.014 %), which confirms its efficiency, robustness, and constraint compliance.
Conclusions: The EMS based on PSO/SAM delivers superior solution quality and processing times in both modes of operation. In GON mode, it reduces the mean costs by 0.0287 % compared to the VSA and 0.2252 % *vs.* the CBGA, whereas, in GOFF mode, the reductions are 0.0191 and 0.0355 %, respectively. These results reflect a more effective cost reduction than exact methods, which constitutes this paper's main contribution.
Keywords: energy management system, battery energy storage, microgrids, swarm optimization, grid-on, grid-off

Article history

Received: 18th/March/2025

Modified: 14th/April/2025

Accepted: 23th/July/2025

Ing, vol. 30, no. 2, 2025. e23474

*Correspondence: grisales.luis@correounivalle.edu.co

Resumen

Contexto: En este artículo se propone un sistema de gestión energética (EMS) para sistemas de almacenamiento de energía en baterías (BESS) orientado a la reducción de costos operativos en microrredes (MG) AC que operan conectados a la red (GON) y en modo isla (GOFF), considerando los costos de compra de energía, generación convencional y mantenimiento a la vez que se cumple con todas las restricciones operativas del sistema y sus componentes.
Método: Como estrategia de operación inteligente del sistema de almacenamiento en baterías, se utiliza una metodología maestro-esclavo basada en optimización por enjambre de partículas y un flujo de potencia horario basado en el método de aproximaciones sucesivas (SAM). Esta propuesta se valida en una MG-AC de 33 nodos, operando en modos GON y GOFF, en comparación con dos métodos alternativos que utilizan el algoritmo de búsqueda por vórtices (VSA) y el algoritmo genético continuo de Chu & Beasley (CBGA) y el mismo método de flujo de potencia.
Resultados: El EMS basado en PSO alcanzó los menores costos, *i.e.*, 6897.59 USD/día (GON) y 17 527.42 USD/día (GOFF), con reducciones en costos del 1.45 y el 0.13 % respectivamente y bajas desviaciones estándar (0.067 y 0.014 %), lo que confirma su eficiencia, robustez y cumplimiento de restricciones.
Conclusiones: El EMS basado en PSO/SAM ofrece una calidad de solución y un tiempo de procesamiento superiores en ambos modos de operación. En el modo GON, reduce los costos promedio en un 0.0287 % en comparación con el VSA y en un 0.2252 % con respecto al CBGA, mientras que, en el modo GOFF, las reducciones son de 0.0191 y 0.0355 % respectivamente. Estos resultados reflejan una reducción de costos más efectiva que la obtenida por métodos exactos, lo que constitye la principal contribución de este artículo.

Palabras clave: sistema de gestión de energía, almacenamiento en baterías, microrredes, optimización por enjambre de partículas, conectado a la red, aislado de la red

Table of contents

Nomenclature

α_j Uniform random value for initialization

β_j Uniform random value for the cognitive component

Δh Time step duration

γ_j Uniform random value for the social component

$\mathbb{S}_d^*$ Conjugate of the complex power demand vector

$\mathbb{V}_d^{t+1}$ Voltage vector of the demand nodes at iteration $t+1$

$\mathbb{V}_d^{t,*}$ Conjugate of the voltage vector of the demand nodes at iteration t

$\mathbb{V}_s$ Voltage vector of the generation (slack) nodes

$\mathbb{Y}_{ds}$ Admittance matrix between the generation and demand nodes

$\mathbb{Z}_{dd}$ Impedance matrix of the demand nodes (inverse of $\mathbb{Y}_{dd}$)

Φ_1 Cognitive acceleration coefficient

Φ_2 Social acceleration coefficient

ϕ_i^B Charge/discharge factor of the BESS at node i

$\theta_{i,h}$ Voltage angle at bus i during time period h

$\theta_{j,h}$ Voltage angle at bus j during time period h

φ_{ij} Admittance angle of the line between buses i and j

C_i^B Nominal capacity of the BESS connected at bus i

$C_{i,h}^{cg}$ Operation and maintenance cost per kW for CG at node i, time h

C_{kWh} Energy purchase cost per kWh at the substation

$C_{O\&M}^b$ BESS operation and maintenance cost

$C_{O\&M}^{dg}$ DG operation and maintenance cost

f_1 Cost of energy purchased at the substation

f_2 Operation and maintenance cost of the BESS and DGs

f_{cost} Total operating cost of the system

$gbest_j$ Global best position in dimension j

$I_{ij,h}$ Current magnitude in line ij at time h

$I_{ij}^{\text{máx}}$ Maximum current in line ij

$Iner_{max}$ Maximum inertia weight

$Iner_{min}$ Minimum inertia weight

$Inertia^{(t)}$ Inertia weight at iteration t

n_s Number of particles

n_v Number of variables (dimensions)

$P_{B,i}^{charg\_\text{máx}}$ Minimum BESS power of charge at node i

$P_{B,i}^{disch\_\text{máx}}$ Maximum BESS power of discharge at node i

$P_{i,h}^B$ Active power from BESS at node i and time h

$P_{i,h}^d$ Active demand at node i and time h

$P_{i,h}^{cg,\text{máx}}$ Maximum active power from CG at node i

$P_{i,h}^{cg,\text{mín}}$ Minimum active power from CG at node i

$P_{i,h}^{cg}$ Active power from CG at node i and time h

$P_{i,h}^{dg,\text{máx}}$ Maximum active power from DG at node i

$P_{i,h}^{dg,\text{mín}}$ Minimum active power from DG at node i

$P_{i,h}^{dg}$ Active power from DG at node i and time h

P_j Active demand at receiving node j.

$pbest_{k,j}$ Personal best position of particle k in dimension j

$Q_{i,h}^d$ Reactive demand at node i and time h

$Q_{i,h}^{cg,\text{máx}}$ Maximum reactive power from CG at node i

$Q_{i,h}^{cg,\text{mín}}$ Minimum reactive power from CG at node i

$Q_{i,h}^{cg}$ Reactive power from CG at node i and time h

Q_j Reactive demand at receiving node j

R_{ij} Resistance of line ij

$SoC_i^{B,\text{máx}}$ Maximum SoC of the BESS at node i

$SoC_i^{B,\text{mín}}$ Minimum SoC of the BESS at node i

SoC_i^f	Final SoC of the BESS at node i
SoC_i^i	Initial SoC of the BESS at node i
$SoC_{i,h}^b$	BESS state of charge at node i and time h
t_{max}	Maximum number of iterations
tc_i^B	BESS charging time at node i
td_i^B	BESS discharging time at node i
$V_i^{\text{máx}}$	Maximum voltage at node i
$V_i^{\text{mín}}$	Minimum voltage at node i
$v_{i,h}$	Voltage magnitude at node i and time h.
$vel_{k,j}^{(t)}$	Velocity of particle k in dimension j at iteration t
Vel_{max}	Maximum velocity bound
Vel_{min}	Minimum velocity bound
$x_j^{\text{máx}}$	Upper bound of the search space in dimension j
$x_j^{\text{mín}}$	Lower bound of the search space in dimension j
X_{ij}	Reactance of line ij
$x_{k,j}^{(t)}$	Position of particle k in dimension j at iteration t
Y_{ij}	Admittance of the line between buses i and j
AC	Corriente alterna
AEA	Algoritmo evolutivo avanzado
BESS	Sistema de almacenamiento de energía en baterías
CB	Algoritmo genético de Chu y Beasley
CBGA	Algoritmo genético de Chu y Beasley continuo
CG	Generadores convencionales
CSA	Algoritmo de búsqueda del cuco
DER	Recurso energético distribuido
DG	Generador distribuido
DRPC	Control directo de potencia reactiva
EMS	Sistema de gestión de energía
EPM	Empresas Públicas de Medellín
GOFF	Modo desconectado de la red (modo isla)
GON	Modo conectado a la red
GWO	Algoritmo de optimización del lobo gris
MG	Microrred
MPPT	Seguimiento del punto de máxima potencia
NTC	Norma Técnica Colombiana
OLGWO	Optimización de lobo gris con aprendizaje por oposición
PPSO	Optimización por enjambre de partículas en paralelo
PSO	Optimización por enjambre de partículas
PV	Fotovoltaico
SA	Método de aproximaciones sucesivas
SDP	Programación semidefinida
SoC	Estado de carga
VSA	Algoritmo de búsqueda por vórtices

1. Introduction

In the last decade, alternating current (AC) microgrids (MG) have been increasingly adopted due to their advantages over conventional grids (1,2). These advantages include the integration of multiple renewable energy sources, an improved control of power demand, and the incorporation of battery energy storage systems (BESS) to manage power surplus (3). AC-MGs also allow for interconnection with conventional grids, creating opportunities to enhance the technical, economic, and environmental performance of electrical systems (4,5).

In recent years, numerous studies have focused on the optimal operation of distributed energy resources (DERs), aiming to reduce the operating costs associated with energy production or purchasing from conventional generators (CG), as well as the maintenance costs related to DERs. These methods enable the optimal coordination of distributed generators (DGs) by minimizing operating costs while satisfying technical constraints in both their grid-connected and standalone modes of operation. However, when energy management strategies focus solely on generation control without integrating energy storage coordination, a considerable amount of surplus energy is wasted. This energy could otherwise be stored and used during peak demand periods, thereby improving MG efficiency and further lowering their operating costs (6,7).

In the context of energy management systems (EMS) for BESS in AC-MGs, several studies in the specialized literature have sought to reduce operating costs. One such example is presented in (8), which employs the opposition-based learning grey wolf optimizer (OLGWO) to enhance the operation of MGs with both renewable and non-renewable DG. This approach, which seeks to minimize operating costs, is benchmarked against the particle swarm optimizer (PSO), the cuckoo search algorithm (CSA), the grey wolf optimizer (GWO), and the gradient-based grey wolf optimizer (GGWO), demonstrating superior convergence speed and solution quality. However, this approach is only evaluated under grid-connected conditions, without considering standalone operation, which limits its validation in real-world scenarios – where MGs must operate in both modes.

The research presented in (9) addresses the problem of EMS for BESS in urban and rural AC distribution networks, with the objective of improving the economic performance of the grid. A mathematical model is developed to minimize operating costs while considering the technical constraints typical of AC networks, including those related to maximum power point tracking photovoltaic (PV) operation and BESS. The proposed solution follows a master–slave strategy, employing metaheuristic methods such as the vortex search algorithm (VSA), PSO, and the continuous genetic-based algorithm (CBGA) in combination with a successive approximations-based hourly power flow algorithm. The model was tested on two Colombian distribution networks — one in grid-connected mode and the other in islanded mode — using real generation and demand data. According to the results, the proposed methodology outperforms PSO and CBGA in terms of solution quality, repeatability, and processing times. However, the issue of parameter tuning is not properly addressed, which limits the performance of otherwise efficient techniques like PSO. To fully exploit the capabilities of each method, a deep and systematic tuning process is essential. Furthermore, although the study considers both grid-connected and islanded operation, it focuses exclusively on static active network scenarios, without evaluating real MG dynamics, where mode transitions may occur due to faults or grid disconnections. In this vein, control strategies must be robust and adaptable to ensure optimal performance under realistic and dynamic operating conditions.

In (9), convex optimization is used within an EMS for AC grids aimed at the optimal dispatch of BESS and renewable sources. Although effective, the use of exact methods like semi-definite programming increases solution complexity and limits adaptability to different scenarios. In contrast, metaheuristic strategies, when properly tuned, can achieve a solution quality comparable to simpler

processes requiring lower computational effort. Their ability to deliver consistent results with low standard deviation values makes them a practical alternative to exact methods in real-world applications.

In (10), a comprehensive economic strategy is proposed for voltage regulation in distribution networks with high PV penetration while integrating BESS and electric vehicles (EV). The objective function aims to maximize the total revenue through the joint management of electricity rates, DERs, and participation in the electricity market. The methodology follows a master–slave model comprising two stages: i) day-ahead forecasting using a hybrid pelican optimization algorithm–XGBoost strategy for the PV output and ii) real-time operation through PSO-based multi-objective optimization. This model was validated on an IEEE 33-bus test network, comparing scenarios with different EV and BESS configurations. Significant economic savings and improvements in voltage quality were achieved. Nevertheless, a key limitation of this study is its assumption of a continuous grid connection, failing to assess system behavior in islanded mode. This restricts the evaluation of operational autonomy and the MG's resilience under external contingencies.

The authors of (11) present an EMS for active distribution networks using BESS. Their objective function aims to minimize the hourly active power losses of the network while considering operating costs and economic benefits. The methodology employs an advanced evolutionary algorithm (AEA) based on genetic principles to optimize the siting, sizing, and coordinated dispatch of BESS alongside distributed wind generation. This approach was validated on an IEEE radial 33-bus distribution system under four scenarios, assessing different configurations with and without BESS and wind integration. The results show that the combined incorporation of BESS and wind resources can reduce network losses by up to 57.2 %, in addition to enhancing voltage stability. However, this research is limited to grid-connected systems and does not explicitly consider autonomous or islanded operation, which restricts its applicability to MG with high levels of operational independence.

The work by (12) develops an EMS for hybrid MGs integrating multiple renewable energy sources and storage technologies, with a focus on ensuring service continuity and improving power quality. The system's implicit objective is to minimize power fluctuations and maximize operational efficiency through DC voltage regulation and the intelligent, sequential use of available energy resources. The control strategy combines fuzzy logic techniques with direct reactive power control (DRPC), employing multilevel converters for the rotors of doubly-fed induction generators (DFIG). This system was validated through MATLAB/Simulink simulations under two configurations: one using batteries and supercapacitors to smooth active power fluctuations and another incorporating an electrolyzer and fuel cell for hydrogen storage and energy recovery during shortfalls. The results show significant improvements in voltage regulation and a reduction in transient stress within the system. However, this study assumes a continuous connection to the main grid and does not explore a fully islanded operation, which limits its applicability in autonomous MG6 environments.

In recent years, several studies have proposed EMS for the optimal operation of BESS in AC-MGs (13). Most of these works focus on minimizing operating costs through a variety of solution methodologies, including convex optimization, metaheuristic techniques, linear programming, and

commercial software tools (14–16). This study aims to maximize the benefits of BESS while achieving the lowest possible operating costs and ensuring consistent performance with minimal standard deviation values and reduced processing times at each execution. The literature emphasizes the effectiveness, robustness, and simplicity of metaheuristic approaches in the implementation of EMS, as they significantly reduce system complexity and deployment costs compared to commercial software. Therefore, metaheuristic optimization methods were adopted in this paper as the core solution strategy.

Table **I** summarizes the methodologies reviewed in the state of the art regarding EMS for BESS in AC-MGs. As shown in Table **I**, the most recent studies on EMS with BESS in AC-MGs focus on grid-connected scenarios, primarily employing metaheuristic or hybrid methodologies to optimize economic objective functions. While significant progress has been made in terms of computational efficiency and solution quality, a notable gap remains in the evaluation of energy management strategies under islanded operating conditions or during dynamic transitions between modes.

Recognizing the current need to develop effective EMS for BESS scheduling in AC-MGs, this work proposes a robust methodology focused on minimizing operating costs through the use of highly efficient metaheuristic techniques. A distinctive feature of the proposed approach is the incorporation of a systematic tuning procedure, which ensures the optimal performance of the optimization algorithm in both grid-connected (GON) and islanded (GOFF) operating modes.

The core of the proposed methodology is the PSO, which is employed to determine the optimal dispatch of BESS. To solve the hourly power flow, the successive approximations (SA) method was selected, given its proven compatibility with metaheuristic optimization. Crucially, the PSO was fine-tuned through a dedicated parameter calibration process, designed to enhance its convergence properties and solution robustness (17, 18). To ensure a fair and comprehensive comparison, two additional algorithms, *i.e.*, the VSA and the CBGA, were also subjected to the same tuning procedure and evaluated under identical conditions using the SA power flow method. This comparative framework allowed for a rigorous assessment of each algorithm's performance under both GON and GOFF conditions.

Validation was carried out on a 33-bus test feeder incorporating real-world generation and demand profiles from the city of Medellín, Colombia. The test system considered the presence of PV generation operating in maximum power point tracking mode in all scenarios. Meanwhile, in the GOFF mode, a diesel generator was included to support the energy supply during low-generation periods. This setup allowed evaluating the EMS under realistic and dynamic MG conditions.

For each method and scenario, 100 independent simulations were performed to evaluate the best-case and average performance, the standard deviation, and the computation time required. The results clearly demonstrate that the proposed PSO-based strategy delivers the most cost-effective solutions, achieving superior performance across all metrics and modes of operation. These findings directly address a gap in the literature, which often limits the analysis to static or GON conditions without evaluating transition dynamics or GOFF performance.

Table I. Comparative summary of recent studies on EMS with BESS in AC-MGs

Reference	Year	Objective function	Solution methodology	Test system or network	Mode of operation
Rajagopalan *et al.* (8)	2022	Minimize operating costs	OGGWO	Single-bus MG	Grid-connected
Grisales *et al.* (9)	2023	Minimize operating costs	Master–slave approach: VSA, PSO, CBGA + successive approximations hourly power flow	33-bus network	Grid-connected
Yan *et al.* (10)	2024	Maximize economic profit	pelican optimization algorithm–XGBoost for forecasting + multi-objective PSO	33-bus network	Grid-connected
Alexprabu and Sathiyasekar (11)	2023	Minimize active losses and operating costs	AEA	33-bus network	Grid-connected
Sahri *et al.* (12)	2021	Minimize power fluctuations and improve power quality	DRPC + fuzzy logic, multilevel converters	Single-bus MG	Grid-connected
Fagundes *et al.* (13)	2024	Minimize operating costs	Fuzzy Logic	Single-bus network	Grid-connected
Wang *et al.* (14)	2024	Minimize production costs	Neural-fuzzy optimization	–	Grid-connected
Nebuloni *et al.* (15)	2023	Profit maximization	GAMS CPLEX solver	Single-bus network	Grid-connected

From an academic standpoint, this work advances the state of the art by introducing a systematically tuned metaheuristic approach for BESS operation within MGs, which is explicitly validated in both GON and GOFF configurations. The study not only confirms the importance of algorithm tuning – often neglected in previous research – but also shows that such calibration significantly improves convergence stability, repeatability, and solution quality when compared to other commonly used metaheuristics.

From an industry perspective, the proposed EMS provides a practical and scalable solution for modern distribution networks with a high penetration of renewable energy and BESS. Its validation with real demand and generation data confirms its applicability in real-world settings, particularly in regions with frequent service interruptions or limited grid infrastructure. The system's ability to maintain optimal performance under diverse and realistic conditions enhances its robustness and makes

it a valuable tool for operational planning and cost-effective energy management in contemporary power systems

The remainder of this document is organized as follows. Section 2 presents the mathematical model for AC-MGs operating in GON and GOFF modes, which aims to reduce operating costs by integrating the full set of constraints that represent AC-MGs in the presence of DERs. Section 3 describes the proposed master-slave methodology, based on PSO and SA, as well as the methods used for comparison and the optimizer parameters obtained through a smart selection process. Section 4 describes the test system used for validation, and Section 5 presents the simulation results. Finally, Section 6 outlines the conclusions of this research, as well as some proposals for future work.

2. Mathematical formulation

The objective of the proposed model is to minimize the total operating cost of an AC-MG over a daily planning horizon. This cost includes both energy purchasing from conventional generators, the operation and maintenance (O&M) costs of DGs and BESS, and the production cost of the diesel generators used in GOFF mode. Our mathematical model is based on the work by (19).

The total operating cost is defined in Eq. (1) as the sum of two components: f_1, the cost of the energy purchased or produced from conventional generators, and f_2, the cost associated with the operation of the BESS and DGs installed in the MG.

$$\text{mín}\left(f_{\text{cost}}\right) = \text{mín}\left(f_1 + f_2\right) \tag{1}$$

The first component, shown in Eq. (2), corresponds to the total energy purchasing or production cost. Here, C_{kWh} is the average energy price in monetary units per kilowatt-hour, $P_{i,h}^{cg}$ represents the active power supplied by the conventional generator at node i during period h, $C_{i,h}^{cg}$ is the variable cost of energy production at node i and hour h, and Δh is the length of each time period (typically one hour).

$$f_1 = C_{\text{kWh}} \sum_{h\in\mathcal{H}} \sum_{i\in\mathcal{N}} P_{i,h}^{cg} C_{i,h}^{cg} \Delta h \tag{2}$$

The second component, presented in Eq. (3), aggregates the O&M costs. Its first term considers the cost associated with the energy charged or discharged by the BESS, where $C_{\text{O\&M}}^{B}$ is the maintenance cost per unit of energy, and $P_{i,h}^{B}$ represents the active power (positive for discharge, negative for charge) from the BESS at node i and hour h. The second term captures the cost of energy produced by DGs, with $C_{\text{O\&M}}^{dg}$ being the O&M cost per kilowatt-hour and $P_{i,h}^{dg}$ the power generated by the DG at node i and hour h.

$$f_2 = C_{\text{O\&M}}^{B} \sum_{h\in\mathcal{H}} \sum_{i\in\mathcal{B}} \left|P_{i,h}^{B}\right| \Delta h + C_{\text{O\&M}}^{dg} \sum_{h\in\mathcal{H}} \sum_{i\in\mathcal{N}} P_{i,h}^{dg} \Delta h \tag{3}$$

The system's operation is subject to several technical constraints. For instance, Eq. (4) ensures the active power balance at each node i and hour h. Its left-hand side represents the sum of all active power sources: conventional generation $P_{i,h}^{cg}$, DG $P_{i,h}^{dg}$, and BESS power $P_{i,h}^{B}$, minus the active load demand $P_{i,h}^{d}$. The right-hand side models the power flow using the polar form, where $v_{i,h}$ and $v_{j,h}$ are voltage

magnitudes at nodes i and j, Y_{ij} is the magnitude of the admittance between nodes i and j, $\theta_{i,h}$ and $\theta_{j,h}$ are voltage angles, and φ_{ij} is the admittance phase angle.

$$P_{i,h}^{cg} + P_{i,h}^{dg} \pm P_{i,h}^{B} - P_{i,h}^{d} = v_{i,h} \sum_{j \in \mathcal{N}} Y_{ij} v_{j,h} \cos(\theta_{i,h} - \theta_{j,h} - \varphi_{ij}) \tag{4}$$

Eq. (5) models the reactive power balance. Here, $Q_{i,h}^{cg}$ and $Q_{i,h}^{d}$ denote the reactive power generated and demanded at node i and hour h, respectively.

$$Q_{i,h}^{cg} - Q_{i,h}^{d} = v_{i,h} \sum_{j \in \mathcal{N}} Y_{ij} v_{i,h} \sin(\theta_{i,h} - \theta_{j,h} - \varphi_{ij}) \tag{5}$$

Eqs. (6) and (7) impose lower and upper bounds on the active and reactive power outputs of conventional generators, respectively. The limits $P_i^{cg,\text{mín}}, P_i^{cg,\text{máx}}, Q_i^{cg,\text{mín}}$, and $Q_i^{cg,\text{máx}}$ represent technical constraints based on generator capacity.

$$P_i^{cg,\text{mín}} \leq P_{i,h}^{cg} \leq P_i^{cg,\text{máx}} \tag{6}$$

$$Q_i^{cg,\text{mín}} \leq Q_{i,h}^{cg} \leq Q_i^{cg,\text{máx}} \tag{7}$$

When the AC-MG operates in GOFF mode, additional constraints must be included to properly represent the behavior of the diesel generator. In this mode, the system cannot export or absorb power, so the generator can only supply energy to the MG.

$$0 \leq P_{i,h}^{\text{cg}}, \tag{8}$$

Furthermore, if the generator is in operation, it must comply with minimum and maximum technical limits, which are defined as a percentage of its nominal capacity, *i.e.*, 40 and 80 % of the nominal power (20). These constraints ensure an efficient and safe operation, preventing inefficient or unsafe conditions while helping to preserve the equipment's lifespan.

Eq. (9) defines the bounds for the DGs. Here, G_h^{dg} is a normalized solar irradiance coefficient (in p.u.) for hour h, which is used to scale the maximum power output $P_i^{dg,\text{máx}}$.

$$P_i^{dg,\text{mín}} \leq P_{i,h}^{dg} \leq P_i^{dg,\text{máx}} G_h^{dg} \tag{9}$$

Eq. (10) ensures that the BESS operate within their charging and discharging power limits, which are denoted by $P_{B,i}^{charg\_max}$ and $P_{B,i}^{disch\_max}$.

$$P_{B,i}^{charg\_max} \leq P_{i,h}^{B} \leq P_{B,i}^{disch\_max} \tag{10}$$

The maximum discharging and charging power of the BESS at node i is defined in Eqs. (11) and (12) as a function of the BESS capacity C_i^B and its corresponding discharging (td_i^B) and charging (tc_i^B) times.

$$P_{B,i}^{disch\_max} = \frac{C_i^B}{td_i^B} \tag{11}$$

$$P_{B,i}^{charg\_max} = -\frac{C_i^B}{tc_i^B} \tag{12}$$

The voltage and current constraints are expressed by Eqs. (13) and (14), where V_i^{min}, V_i^{max} denote the voltage limits and I_{ij}^{max} is the maximum current flowing through line ij.

$$V_i^{min} \leq v_{i,h} \leq V_i^{max} \tag{13}$$

$$|I_{ij,h}| \leq I_{ij}^{max} \tag{14}$$

The state of charge (SoC) of each BESS is dynamically updated using Eq. (15), where ϕ_i^B represents an efficiency-based coefficient and Δt is the time step.

$$SoC_{i,h}^B = SoC_{i,h-1}^B - \phi_i^B P_{i,h}^B \Delta t \tag{15}$$

The charge/discharge coefficient ϕ_i^B, shown in Eq. (16), depends on capacity and maximum power ratings of the BESS (21).

$$\phi_i^B = \frac{1}{td_i^B P_{B,i}^{disch\_max}} = \frac{1}{tc_i^B P_{B,i}^{charg\_max}} \tag{16}$$

The initial and final SoC are set using Eqs. (17) and (18). The SoC must always stay within the predefined minimum and maximum limits, as shown in Eq. (19).

$$SoC_{i,0}^B = SoC_i^i \tag{17}$$

$$SoC_{i,24}^B = SoC_i^f \tag{18}$$

$$SoC_i^{B,min} \leq SoC_{i,h}^B \leq SoC_i^{B,max} \tag{19}$$

3. Solution methodology: PSO/SAM

This study employs a master–slave methodology that combines the PSO and the successive approximations method (SAM) to determine the optimal operation of BESS in AC-MGs that incorporate PV generators operating at their maximum power point. PSO is responsible for determining the BESS operation schedule over a 24-hour horizon, while SAM solves the power flow, evaluating the objective function and the constraints associated with each possible BESS operating condition within the MG.

3.1. Master stage: PSO

This work proposes a solution method based on PSO to determine the optimal operation of BESS in AC-MGs (22). PSO is a population-based metaheuristic inspired by the coordinated movement of bird flocks or fish schools. In each iteration, the algorithm updates the position of each particle using both individual knowledge (the best solution found by the particle) and social knowledge (the best solution found by the entire population) (23, 24).

The algorithm starts by defining all the relevant parameters, *i.e.*, the number of particles (n_s), the number of variables (n_v), the maximum number of iterations (t_{max}), the inertia limits ($Iner_{max}$,

$Iner_{min}$), the cognitive and social factors (Φ_1, Φ_2), and the velocity bounds (Vel_{min}, Vel_{max}). Each particle is initialized randomly within the search space:

$$x_{k,j}^{(1)} = x_j^{\text{mín}} + \alpha_j \cdot (x_j^{\text{máx}} - x_j^{\text{mín}}), \tag{20}$$

$$vel_{k,j}^{(1)} = Vel_{min} + \alpha_j \cdot (Vel_{max} - Vel_{min}), \tag{21}$$

where $\alpha_j \sim \mathcal{U}(0,1)$ for $k = 1, \ldots, n_s$ and $j = 1, \ldots, n_v$. In the optimal BESS operation problem, each particle in the PSO represents a candidate solution, whose position corresponds to the charging or discharging power levels of the BESS installed in the AC-MG.

BESS 1					**BESS 2**					**BESS 3**				
h=1	**h=2**	⋯	**h=23**	**h=24**	**h=1**	**h=2**	⋯	**h=23**	**h=24**	**h=1**	**h=2**	⋯	**h=23**	**h=24**
0.5	0.72	⋯	0.34	0.5	0.5	0.61	⋯	0.83	0.5	0.5	0.27	⋯	0.49	0.5

Figure 1. Encoding used to generate a solution for operation of BESS in AC-MGs

Fig. 1 presents the encoding used to represent the 24-hour operating profile of each BESS. Each row corresponds to a BESS and is divided into hourly intervals. The values represent the normalized power levels for charging or discharging at each time step. The first and last hours are highlighted to reflect boundary conditions, assuming an initial and final SoC of 50 %, as per IEEE recommendations (9). This structure allows the PSO to evaluate each particle as a complete and feasible operation schedule for the BESS.

Once the initial population has been generated, the objective function is evaluated for each particle using the SAM described in slave stage. The initial position of each particle becomes its personal best, and the best solution among all particles is set as the global best.

In each iteration t, the inertia coefficient is linearly updated.

$$Inertia^{(t)} = Iner_{max} - \frac{(Iner_{max} - Iner_{min}) \cdot t}{t_{max}}. \tag{22}$$

The PSO's velocity update equation determines how each particle adjusts its trajectory within the solution space. For each particle k and each dimension j, the updated velocity at iteration t, denoted as $vel_{k,j}^{(t)}$, is calculated as follows:

$$\begin{aligned} vel_{k,j}^{(t)} = {} & Inertia^{(t)} \cdot vel_{k,j}^{(t-1)} + \beta_j \cdot \Phi_1 \cdot (pbest_{k,j} - x_{k,j}^{(t-1)}) \\ & + \gamma_j \cdot \Phi_2 \cdot (gbest_j - x_{k,j}^{(t-1)}), \end{aligned} \tag{23}$$

This expression consists of three components. The first term, $Inertia^{(t)} \cdot vel_{k,j}^{(t-1)}$, represents the inertia component, which preserves part of the previous velocity to maintain the particle's momentum. The second term, $\beta_j \cdot \Phi_1 \cdot (pbest_{k,j} - x_{k,j}^{(t-1)})$, is the cognitive component, which drives the particle toward its own best-known position. Here, Φ_1 denotes the cognitive acceleration coefficient, and β_j is a

uniformly distributed random number in the interval $[0, 1]$. The third term, $\gamma_j \cdot \Phi_2 \cdot (gbest_j - x_{k,j}^{(t-1)})$, is the social component, which attracts the particle towards the best position found by the entire swarm. Here, Φ_2 is the social acceleration coefficient, and γ_j is another random value in $[0, 1]$. Together, these three components balance exploration and exploitation, allowing the swarm to converge towards optimal or near-optimal solutions (25).

Once the velocity has been updated, the new position of each particle is calculated by means of the following equation:

$$x_{k,j}^{(t)} = x_{k,j}^{(t-1)} + vel_{k,j}^{(t)}. \tag{24}$$

In this expression, $x_{k,j}^{(t)}$ represents the updated position of particle k in dimension j at iteration t. This is obtained by adding the newly computed velocity $vel_{k,j}^{(t)}$ to the particle's previous position $x_{k,j}^{(t-1)}$. This operation allows the particle to move through the solution space, guided by the influence of its own experience and the collective knowledge of the swarm. This step is essential for exploring new candidate solutions and gradually approaching the global optimum.

In this study, the velocity and position of each particle are updated while ensuring that they remain within the feasible operating range. Specifically, the power values associated with each particle are limited according to the maximum charging and discharging capabilities specified in the datasheet of the BESS under consideration.

After evaluating the objective function and constraints of the new positions using the slave stage, the personal best of each particle and the global best of the swarm are updated if better solutions are found. The algorithm stops when it reaches a predefined maximum number of iterations. The best solution found is returned as the optimal BESS schedule. A summary of the parallel PSO (PPSO) is presented in Fig. 2, which illustrates the main steps and structure of the proposed approach.

3.2. Slave stage: SAM

In our proposal's master stage, the PSO generates candidate operation schedules for the BESS over a 24-hour horizon. Each particle represents a potential combination of hourly charging and discharging power values for each BESS.

The slave stage is responsible for evaluating the technical viability and overall performance of each candidate solution provided by the PSO in relation to the objective function and constraints. This is accomplished through a sequential, hour-by-hour power flow analysis using the SAM (26). The selection of this method was based on its excellent performance in terms of convergence and processing times, as it has outperformed both classical and modern approaches such as the Newton-Raphson, Gauss-Seidel, accelerated Gauss-Seidel, Levenberg-Marquardt, and graph-based backward/forward sweep methods.

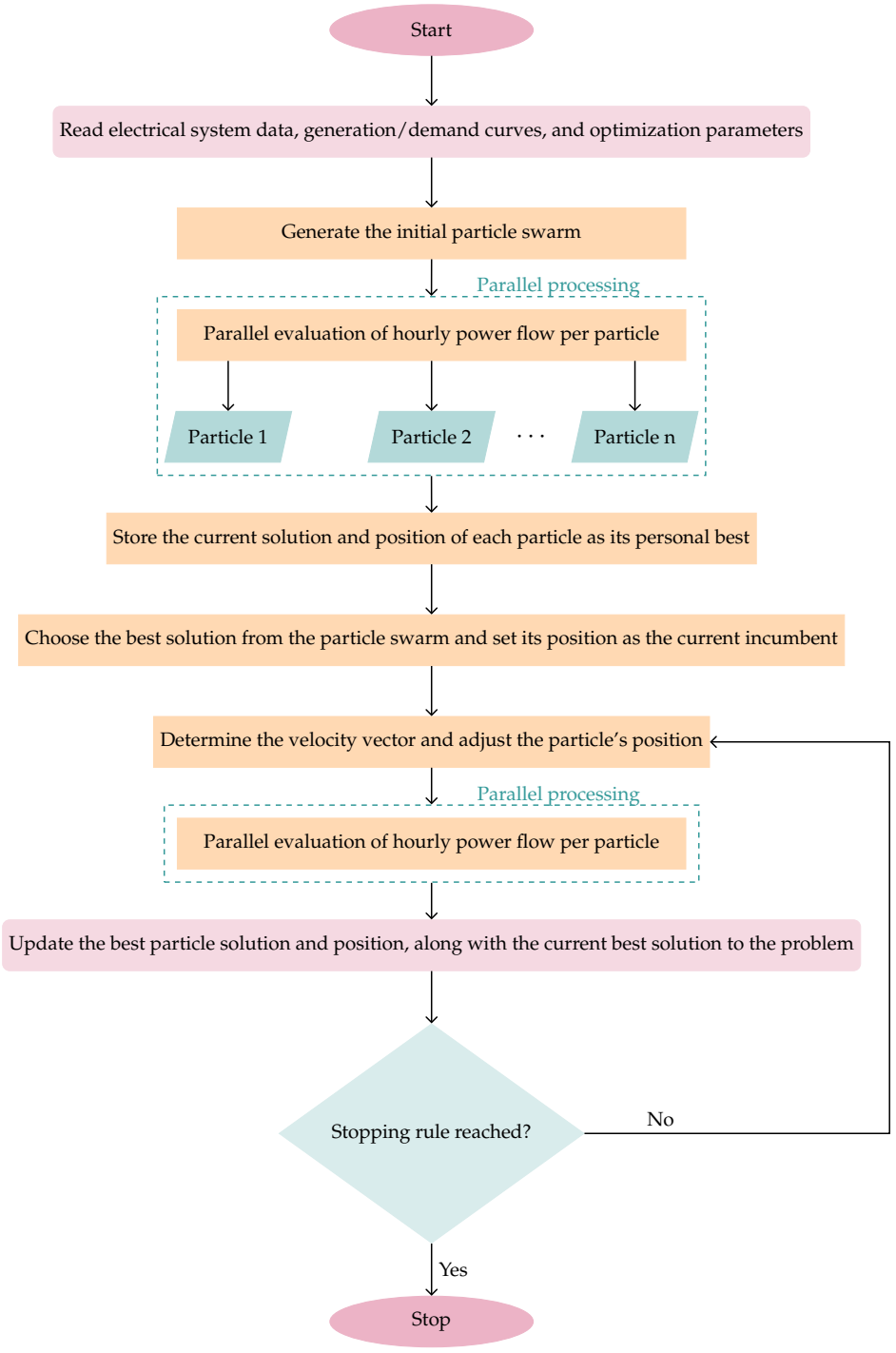

Figure 2. Step-by-step flowchart of our PSO method

The evaluation process follows the steps presented below.

1. **Hourly data setup**: For each hour $h \in \{1, 2, ..., 24\}$, retrieve:
    - The load demand profile

- The power output from PV generation
- The charging/discharging power values of the BESS (provided by the PSO)

2. **Solve the power flow**: Using the SAM, solve the nodal equations to estimate the voltage magnitudes and line flows:

$$\mathbb{V}_{d,h}^{t+1} = -\mathbb{Y}_{dd}^{-1}\left[\mathbb{Y}_{ds}\mathbb{V}_{s,h} + diag^{-1}(\mathbb{V}_{d}^{t,*})\mathbb{S}_{d,h}^{*}\right] \tag{25}$$

3. **Constraint verification**: Check whether the solution satisfies all operational limits, *i.e.*,
   - the voltage magnitude boundaries at each node
   - that the current flows within thermal limits of the lines
   - that the BESS operates within its charge/discharge capacity
4. **Penalty assessment**: If violations are detected, penalty terms are added to the objective function in order to reduce the quality of the solution. To this effect, the fitness function reported in (9) is employed.
5. **Cost aggregation**: Once all 24 hourly scenarios have been evaluated, the total operating cost of the MG is calculated by applying the fitness function, which includes penalties for any constraint violations associated with the proposed schedule.
6. **Feedback for the PSO**: The final fitness value is returned to the master stage (PSO), which uses it to guide the swarm toward more optimal BESS schedules in the next iterations.

This methodology allows for a dynamic evaluation of the MG under various BESS operation scenarios, ensuring that each proposed solution is both technically feasible and economically sound. The SAM offers a computationally efficient approach for solving the power flow equations, while the PSO of BESS schedules enhances voltage regulation, operational reliability, and cost-effectiveness.

4. Test system

For validation purposes, this study used a 33-bus AC-MG as a test system, evaluating its operation in both GON and GOFF modes (27). The analysis considers the variable power generation and demand profiles typical of Medellín, Colombia, based on data reported by the local public utility, Empresas Públicas de Medellín (EPM), and NASA datasets (9). A single-line diagram of the test system is presented in Fig. 3.

The same test system was used for both modes of operation, reflecting practical MG applications where the infrastructure remains unchanged regardless of whether the network is connected to the main grid (28). The key distinction lies in the source providing grid support: the utility grid in GON mode or a local synchronous diesel generator in the GOFF mode (29). Furthermore, using a single system allows for a consistent evaluation of the implemented optimization methodologies, as each mode implies a different solution space. Comparing their performance within the same system ensures that any differences in the results are due to operating conditions rather than changes in the network

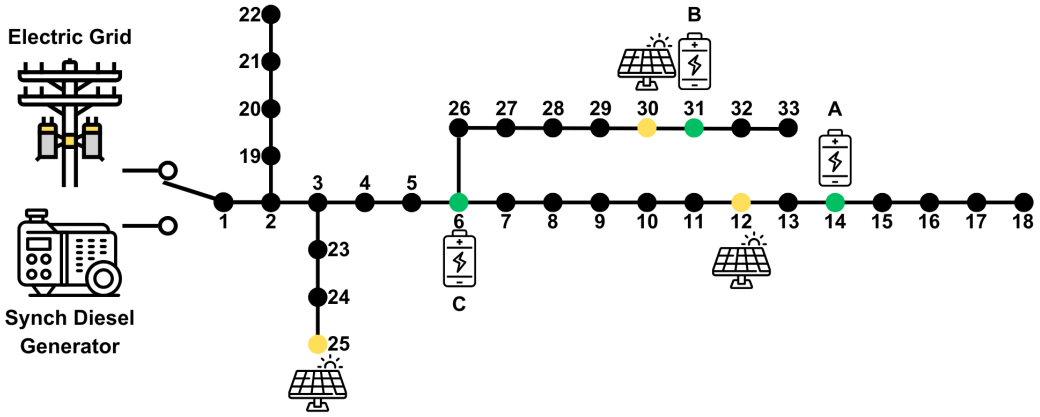

Figure 3. Line diagram of the 33-buses AC-MG used for testing

configuration, enabling a fair analysis in terms of the best and average solutions, the standard deviation, and the computational time required.

The test system operates at a nominal voltage of 12.66 kV and a base power of 100 kW. It consists of 33 buses, 32 distribution lines, and one slack bus, which represents the point of connection to the conventional power grid and the diesel generator used for GOFF operation. The technical parameters of the lines, including the resistance, reactance, load demands, and current limits, are detailed in Table **II**.

The MG includes three PV generators located at buses 12, 25, and 30, with rated capacities of 1125, 1320, and 999 kW, respectively. These units operate in maximum power point tracking (MPPT) mode throughout the simulation period. Fig. **4** shows the typical daily generation and demand curves for Medellín.

Three lithium-ion BESS units are installed at buses 6, 14, and 31. These units are classified into three types: A, B, and C, with nominal capacities of 1000, 1500, and 2000 kWh, respectively. With charging and discharging times of four hours for types A and B and five hours for type C (30). Each BESS operates within a SoC range of 10-90 %, with initial and final values fixed at 50 % to ensure a stable operation and preserve BESS health, as recommended by the IEEE (30).

All bus voltages are required to remain within $\pm 10\,\%$ of the nominal value, in accordance with Colombian technical standards (NTC 1340) (31).

As for the operating costs, two scenarios were considered: a GON case with time-varying energy prices and a GOFF one with fixed generation costs. The hourly variations in energy prices used for the GON scenario are illustrated in Fig. **4**.

Table II. Technical parameters of the 33-bus AC-MG

Line l	Node i	Node j	R_{ij} (Ω)	X_{ij} (Ω)	P_j (kW)	Q_j (kVAr)	$I_{ij}^{\text{máx}}$ (A)
1	1	2	0.0922	0.0477	100	60	385
2	2	3	0.4930	0.2511	90	40	355
3	3	4	0.3660	0.1864	120	80	240
4	4	5	0.3811	0.1941	60	30	240
5	5	6	0.8190	0.7070	60	20	240
6	6	7	0.1872	0.6188	200	100	110
7	7	8	1.7114	1.2351	200	100	85
8	8	9	1.0300	0.7400	60	20	70
9	9	10	1.0400	0.7400	60	20	70
10	10	11	0.1966	0.0650	45	30	55
11	11	12	0.3744	0.1238	60	35	55
12	12	13	1.4680	1.1550	60	35	55
13	13	14	0.5416	0.7129	120	80	40
14	13	15	0.5910	0.5260	60	10	25
15	15	16	0.7463	0.5450	60	20	20
16	16	17	1.2890	1.7210	60	20	20
17	17	18	0.7320	0.5740	90	40	20
18	18	19	0.1640	0.1565	60	40	20
19	19	20	1.5042	1.3554	90	40	20
20	20	21	0.4095	0.4784	90	40	20
21	21	22	0.7089	0.9373	90	40	20
22	3	23	0.4512	0.3083	90	50	85
23	23	24	0.8980	0.7091	420	200	85
24	24	25	0.8960	0.7011	420	200	40
25	6	26	0.2030	0.1034	60	25	125
26	26	27	0.2842	0.1447	60	25	110
27	27	28	1.0590	0.9337	60	20	110
28	28	29	0.8042	0.7006	120	70	110
29	29	30	0.5075	0.2585	200	600	95
30	30	31	0.9744	0.9630	150	70	55
31	31	32	0.3105	0.3619	210	100	30
32	32	33	0.3410	0.5302	60	40	20

Finally, the economic and environmental performance of the MG was assessed using specific cost and emissions parameters. In GON mode, the cost of electricity purchased from the main grid was \$0.1302/kWh, while, in GOFF mode, this value increased to \$0.2913/kWh (32). The operation and maintenance cost of the distributed PVs was estimated at \$0.0019/kWh, and the maintenance costs associated with the BESS was set at \$0.0017/kWh (32). Regarding the environmental impact, the CO_2 emissions were 0.1644 kg/kWh during GON operation and 0.2671 kg/kWh in GOFF scenario (32).

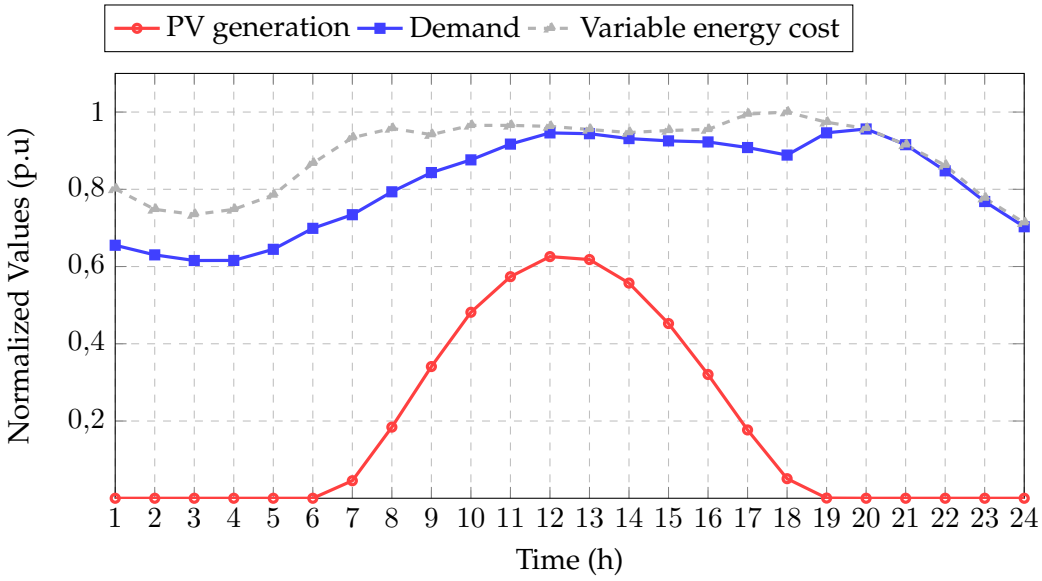

Figure 4. Normalized daily profiles regarding PV generation, energy demand, and variable energy costs for Medellín, Colombia

4.1. Comparison and parameter tuning

All optimization methodologies were calibrated using a PSO configured with 100 particles, whose cognitive and social coefficients were set to 1.494. The inertia weight ranged from a maximum value of 1 to a minimum of 0, and the stopping criterion was set to a maximum of 300 iterations. This algorithm has been extensively used in the literature to enhance energy management strategies in systems integrating DERs (9). Its purpose within this context is to determine the optimal set of parameters that allows each control strategy to achieve its best possible performance (25).

During the tuning process, specific parameter configurations were assigned to each optimization method for both GON and GOFF operating conditions. To apply PSO, the GON scenario was configured with a population of 72 particles and a maximum of 1239 iterations. The inertia weight ranged from 0.8926 to 0.5103, with the cognitive and social factors set to 1.3235 and 0.8236, respectively. A velocity limit factor of 0.2172 was also implemented to constrain particle displacement. For the GOFF case, the configuration used 462 particles, 648 iterations, an inertia weight between 1 and 0.8457, and cognitive and social coefficients of 0.8260 and 0.2978. The velocity limit factor in this case was reduced to 0.0385.

To validate the effectiveness of the PPSO/SAM EMS, comparative analyses were conducted with two alternative metaheuristic approaches: the VSA (33) and CBGA (34), both implemented using the same power flow model (*i.e.*, the SAM).

For the VSA, the GON mode employed 100 individuals and a maximum of 1000 iterations, while the GOFF configuration used 233 individuals and 4000 iterations. The decay rate was adjusted according to the mode of operation, with values of -9.0645 and -11.4285 for GON and GOFF conditions, respectively.

The CBGA was set with ten individuals and 2000 iterations in GON mode, using three mutation operations per generation. In contrast, the GOFF configuration was expanded to 200 individuals and 4000 iterations, with only one mutation per generation.

Finally, in this paper, a parallel processing approach was incorporated into the proposed solution methodologies in order to enhance their performance (*i.e.*, PVSA and PPSO). This parallelization allowed evaluating a larger number of individuals per iteration by utilizing all available workstation cores (35). In other words, multiple power flow analyses were executed in parallel, using the SAM for the different BESS operation schemes proposed by the VSA and PSO, corresponding to a subset of individuals in the population, limited by the number of available workers. This significantly reduced the computation time of the proposed methodologies. Our parallel implementation followed the procedure described in (36–38). However, it was not possible to implement the parallel processing approach in the case of the CBGA due to its characteristics, as it evaluates only one individual per iteration (39).

5. Analysis and discussion

This section analyzes and discusses the simulation results obtained via PPSO and the methods used for comparison. Our EMS for the optimal operation of BESS in AC-MGs was implemented and solved in MATLAB 2024a, using an Asus ROG Strix SCAR 18 (2024) G834 workstation laptop with an Intel Core i9-14900HX processor, an NVIDIA GeForce RTX 4090 GPU, 32 GB of DDR5-5600 RAM, and dual 1 TB PCIe 4.0 NVMe SSDs running Windows 11 Home Edition. Each objective function was analyzed in both MGs, considering the best and average solutions, the standard deviation, and their percentage differences. For statistical validation, each methodology was run 100 times.

This section presents the numerical results obtained with the proposed master-slave optimization scheme. Recall that the performance of this strategy was assessed under two scenarios: GON and GOFF.

The performance metrics considered include the total operating cost, convergence behavior, and computational efficiency. To obtain statistically significant insights regarding the robustness and consistency of each optimization technique, all simulations were executed 100 consecutive times under identical conditions. This approach allowed for a more rigorous evaluation of the computational effort required by each method and the variability in the quality of the solutions obtained. The following subsections detail the simulation setup, present the results for each mode of operation, and provide a comparative analysis of the optimization strategies employed.

5.1. Numerical performance of the proposed methodology

Tables **III** and **IV** summarize the numerical performance of the proposed PPSO/SAM approach when compared against two alternative metaheuristic techniques: the CBGA and the VSA. The performance metrics reported include the best solution, the average solution, the standard deviation (expressed as a percentage of the mean), and the average computational time per run (in seconds). Table

III presents the results for the GON mode, where the MG operates in coordination with the main grid, while Table **IV** reports the outcomes for the GOFF mode, where the system operates autonomously using a diesel generator, PVs, and BESS.

Table III. Numerical results obtained for the 33-bus feeder during GON operation

Obj. funct.	E_{Cost} **(USD/day)**			
Base case	6999.05313			
Methodology	**Best solution**	**Mean solution**	**Std. dev. (%)**	**Mean time (s)**
CBGA	6906.11828	6916.08321	0.07079	2.80158
PVSA	6897.95530	6902.48686	0.08904	39.12587
PPSO	6897.58646	6900.50405	0.06748	39.15777

Table IV. Numerical results obtained for the 33-bus feeder during GON operation

Obj. func.	E_{Cost} **(USD/day)**			
Base case	17550.5832			
Methodology	**Best solution**	**Mean solution**	**Std. dev. (%)**	**Mean time (s)**
CBGA	17533.60244	17535.95161	0.00837	5.53265
PVSA	17527.57720	17533.07184	0.01823	252.09230
PPSO	17527.41548	17529.71611	0.01453	67.90528

Based on the data presented in Tables **III** and **IV**, the following can be stated:

- In GON mode, PPSO achieves the lowest operating cost, with a best solution of 6897.58646 USD/day, outperforming both PVSA (6897.95530 USD/day) and CBGA (6906.11828 USD/day). This represents a cost reduction of approximately 101.47 USD/day compared to the base, non-optimized case (6999.05313 USD/day), demonstrating the substantial economic benefits of the proposed EMS. Additionally, PPSO achieves a reduction of 0.37 USD/day compared to PVSA, as well as 8.53 USD/day compared to CBGA. It is important to highlight that, for the GON case, the proposed methodology clearly outperforms the results reported in (40), where an optimization strategy based on semi-definite programming (SDP) was implemented. In that study, the SDP approach reported an objective function value of 6897.69280 USD/day.

  In GOFF mode, the best solution is again obtained by PPSO (17527.41548 USD/day), surpassing PVSA (17527.57720 USD/day) by 0.16 USD/day and CBGA (17533.60244 USD/day) by 6.19 USD/day. Compared to the base case (17550.5832 USD/day), PPSO yields a total cost reduction of 23.17 USD/day, further confirming its superior performance in standalone operation scenarios.

- The mean solution represents the expected cost over 100 consecutive runs. In GON mode, PPSO yields the lowest average cost (6900.50405 USD/day), followed by PVSA (6902.48686 USD/day) and CBGA (6916.08321 USD/day). PPSO not only finds better individual solutions; it also reaches them more consistently, which is essential for a robust EMS. Similarly, in GOFF mode, the lowest average cost is again achieved by PPSO (17529.71611 USD/day), followed by PVSA

(17533.07184 USD/day) and CBGA (17535.95161 USD/day). This further reinforces PPSO's ability to consistently deliver high-quality solutions across multiple executions.

- In terms of standard deviation, PPSO exhibits the lowest variability in GON mode (0.06748 %), indicating high convergence consistency. In comparison, PVSA (0.08904 %) and CBGA (0.07079 %) show slightly higher deviations, reflecting greater dispersion in their results. The low standard deviation achieved by PPSO confirms its robustness.

  On the other hand, in GOFF mode, CBGA achieves the lowest standard deviation (0.00837 %), indicating high consistency — although this comes at the expense of lower-quality solutions. PPSO maintains a relatively low deviation (0.01453 %), striking a favorable balance between solution quality and reliability. PVSA shows the highest deviation (0.01823 %), indicating greater instability in its outcomes.

- Finally, from a computational standpoint, in GON mode, CBGA is the fastest method (2.80 s), although this comes at the expense of solution quality. PPSO and PVSA exhibit nearly identical runtimes (39.15 s), significantly higher than those of CBGA. However, the superior accuracy and consistency of PPSO justify this moderate computational overhead. In GOFF mode, the computational time varies significantly among the methods. CBGA is again the fastest (5.53 s), making it computationally efficient, albeit with suboptimal results. PVSA is the slowest (252.09 s), which is a considerable drawback,especially given that it does not outperform PPSO. The latter requires an average of 67.91 s, which is acceptable considering its superior performance.

This comparative analysis shows that the proposed methodology consistently outperforms CBGA and PVSA across all evaluated criteria. In both GON and GOFF modes, PPSO achieves the lowest operating costs (corresponding to both the best and mean solutions) while maintaining low variability, indicating strong robustness and convergence. Although CBGA offers the shortest computation time, it sacrifices solution quality. PPSO strikes a well-balanced trade-off between accuracy, reliability, and efficiency, achieving cost reductions of 101.47 USD/day and 23.17 USD/day compared to the base case in GON and GOFF modes, respectively. These results confirm PPSO as an effective and reliable optimization strategy for energy management in MGs under both grid-connected and islanded conditions.

On the other hand, Figs. 5 and 6 illustrate the percent cost reduction achieved by the three metaheuristic methods relative to the base case. The analysis considers both the best and the mean solutions obtained after 100 independent runs of each method. Fig. 5 corresponds to the GON mode, while Fig. 6 presents the results for the GOFF mode, both applied to a modified 33-bus test system.

Both figures confirm that PPSO consistently achieves the highest percentage reduction in operating costs across both modes of operation and performance metrics. In GON mode (Fig. 5), the performance gap is more pronounced, with all three methods achieving reductions above 1 % and PPSO slightly outperforming its competitors. In contrast, Fig. 6 shows that the magnitude of the cost reduction in GOFF mode is significantly lower, with all methods achieving reductions below 0.15 %. This outcome is expected, as operational flexibility is reduced under islanded conditions, limiting the potential benefits

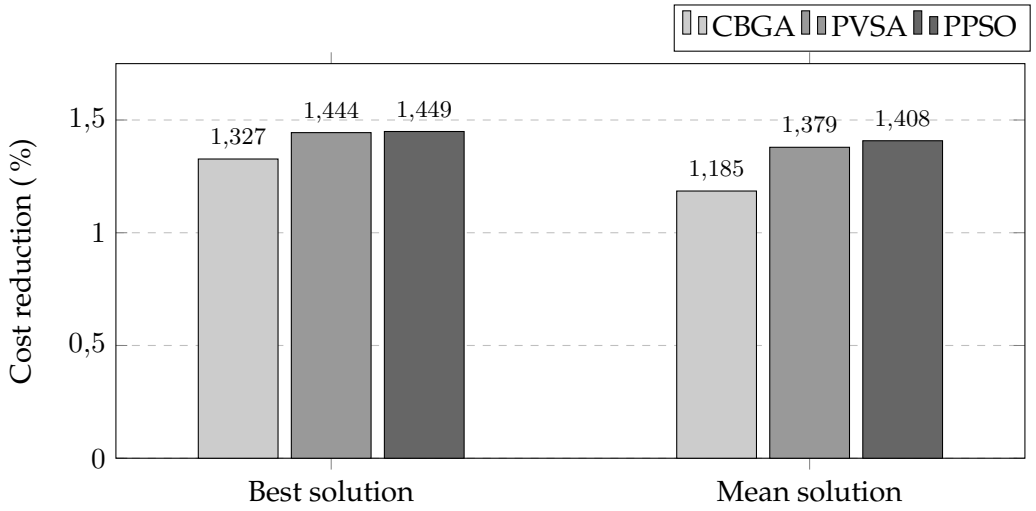

Figure 5. Percent cost reduction by methodology with respect to the base case in the 33-node system during GON operation

of optimization. Nevertheless, PPSO still delivers the best results, demonstrating its adaptability even in constrained environments.

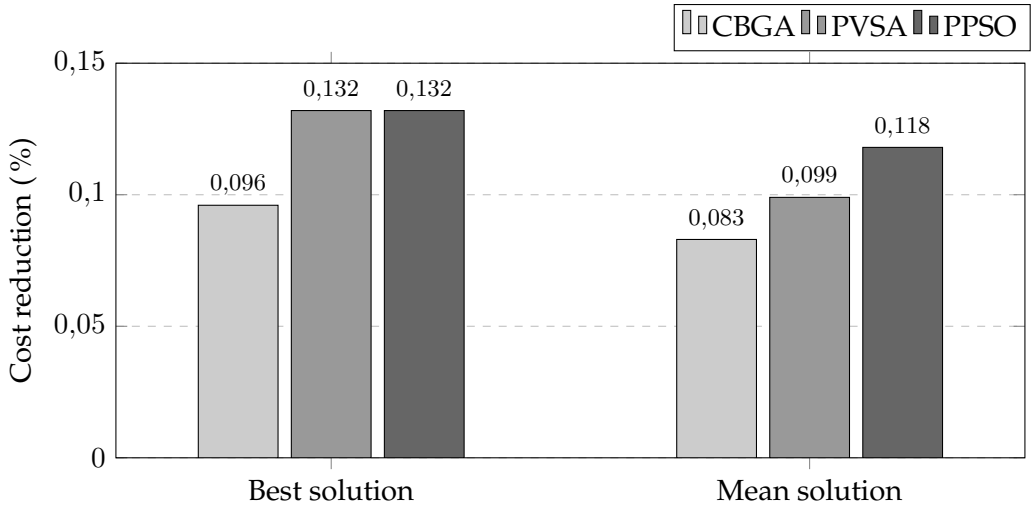

Figure 6. Percent cost reduction by methodology with respect to the base case in the 33-node system during GOFF operation

Figs. **5** and **6** visually reinforce the quantitative findings presented in Tables **III** and **IV**: the PPSO-based EMS outperforms CBGA and PVSA in both operational scenarios. Our proposal's ability to consistently yield the highest percentage reductions — particularly in terms of the average performance — demonstrates not only its effectiveness in minimizing operating costs, but also its robustness and reliability. These figures further validate PPSO as the most balanced and efficient optimization strategy among the evaluated methods for energy management in AC-MGs under both GON and GOFF conditions.

Fig. 7 presents the dispersion diagrams (boxplots) of the objective function E_{Cost} for the metaheuristic methods in both modes of operation: a) GON and b) GOFF. Each boxplot summarizes the distribution of the operating costs over 100 consecutive executions, allowing for a visual inspection of each method's central tendency, spread, and presence of outliers.

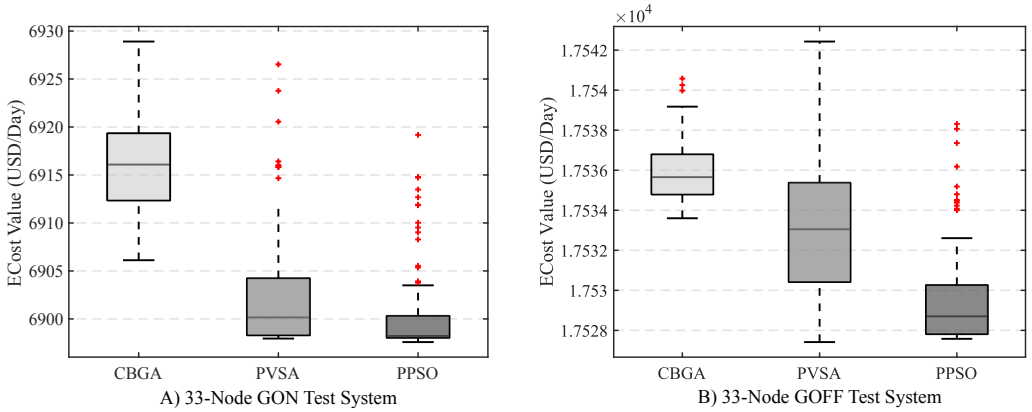

Figure 7. Dispersion diagram of results for E_{Cost}: a) GON and b) GOFF operation

These boxplots provide key insights into each method's robustness and stability. PPSO consistently achieves lower medians and tighter distributions in both GON and GOFF modes, confirming its ability to converge towards high-quality solutions with minimal variability. PVSA, while occasionally competitive in terms of its best solutions, exhibits greater variance and more pronounced outliers, especially in GOFF mode, which suggests a less stable performance. CBGA exhibits a stable but suboptimal behavior, with concentrated yet consistently higher cost values across both modes.

Fig. 7 reinforces the conclusion that PPSO is the most reliable and cost-effective strategy among the evaluated methods. Its low median costs, narrow variability, and controlled dispersion of outliers in both operational scenarios indicate a strong capacity for producing robust and high-quality solutions. In contrast, PVSA and CBGA either lack consistency or deliver less competitive results, underscoring the advantages of the PPSO-based EMS for operating cost minimization in MGs.

5.2. Validating the operational constraints

This section analyzes the results related to the SoC of the BESS (Figs. 8 and 9), the system's nodal voltage profiles (Figure 10), and its line loading levels (Fig. 11) over a typical day of operation. The findings confirm that our EMS allows for feasible MG operation while adhering to the technical limits imposed on storage systems, voltage regulation, and line capacities in both GON and GOFF modes.

Figs. 8 and 9 illustrate the evolution of the SoC for the three BESS (A, B, and C) over a 24-hour period in the two modes of operation. Fig. 8 corresponds to the GON mode, while Fig. 9 represents the GOFF mode. Both figures show the hourly SoC profiles obtained from the optimal solution using the PPSO-based EMS.

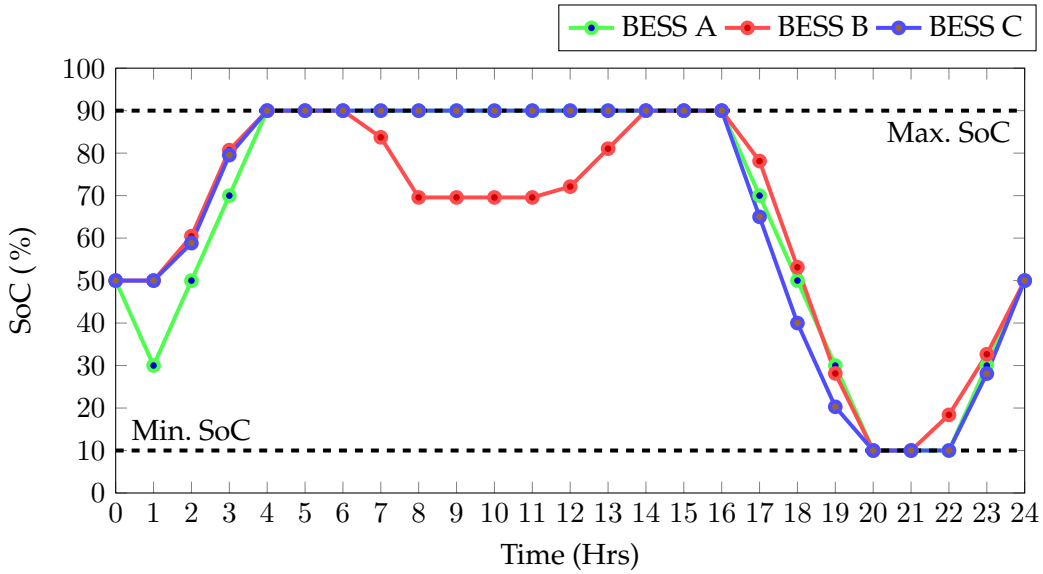

Figure 8. SoC in the optimal solution obtained by the PPSO over a representative day of operation in GON mode

In both figures, the SoC trajectories for each BESS remain within the predefined technical limits, *i.e.*, min. SoC: 10 %; max. SoC: 90 %, and the SoC also starts and ends at the value predefined by the network operator (50 %). In GON mode, the SoC shows greater variability and more aggressive charging and discharging cycles, especially between hours 1 and 5, when the BESS charge to their maximum level, and between hours 16 and 22, when they discharge from maximum to minimum, delivering all their energy to the system. In contrast, under GOFF conditions, the SoC curves are smoother and more conservative, with BESS A and B supplying power to the grid during the first ten hours. Once the solar resource begins injecting its maximum power, the BESS are charged to their maximum level and then discharged down to 50 % of their maximum charge at hour 17.

The behavior observed in GON mode (Fig. 8) reflects the system's ability to take advantage of grid availability, allowing for deeper charge/discharge cycles to optimize operating costs. The BESS charge during the early hours, when both energy prices and demand are at their lowest levels (below 80 %), and begin discharging after hour 16 as energy demand exceeds 90 % and energy prices reach their peak (above 95 %). This indicates that the proposed EMS strategically leverages the variability in energy prices and demand to improve economic performance.

On the other hand, in GOFF mode (Fig. 9), the strategy prioritizes energy conservation, as there is no external grid support. To ensure supply continuity, both the BESS and the diesel generator inject power into the network. Later, when renewable resources become abundant (starting around hour 9) the BESS are charged to their maximum capacity. Finally, as in the GON case, the strategy takes advantage of the fact that both energy prices and demand are at their highest levels during the day to inject power into the system, thereby reducing operating costs.

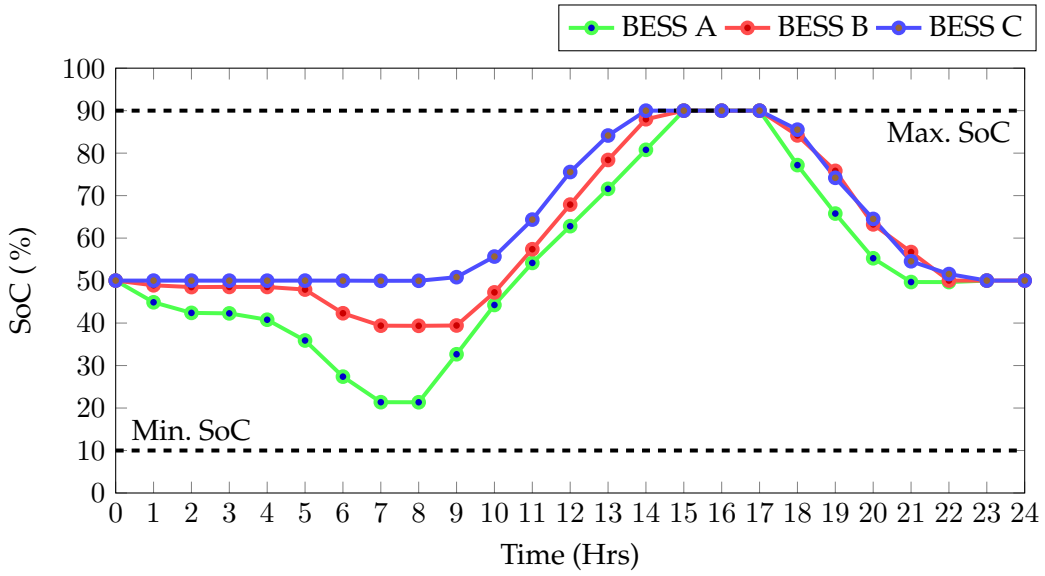

Figure 9. SoC in the optimal solution obtained by the PPSO over a representative day of operation in GOFF mode

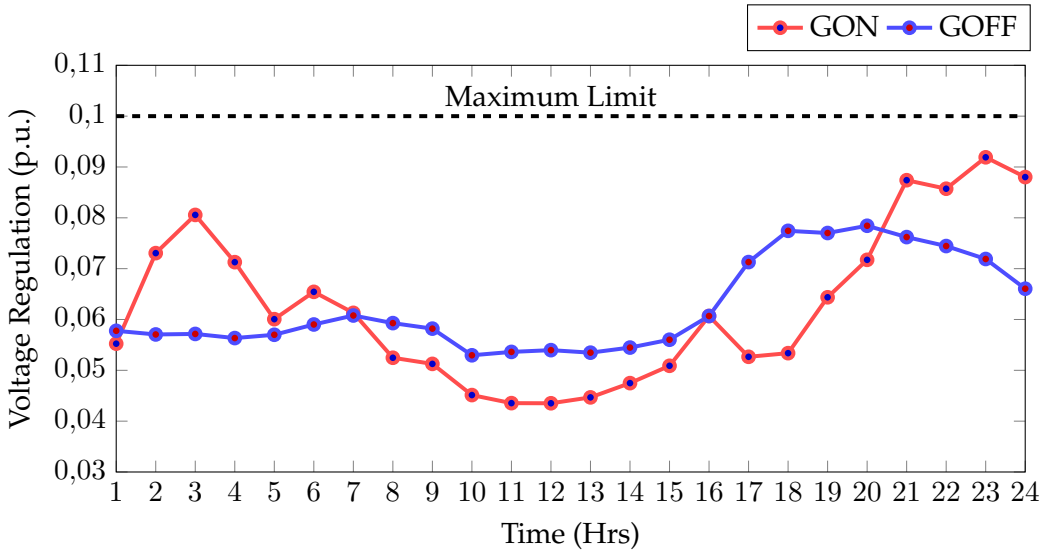

Figure 10. Voltage regulation in the optimal solution obtained by the PPSO for a representative day of operation

Fig. 10 illustrates the voltage regulation performance, expressed in p.u., over a 24-hour period for a representative day of operation. The results are shown for both the GON and GOFF modes, based on the optimal solution obtained using the PPSO-based EMS.

Throughout the day, both the GON and GOFF profiles remain well below the 0.10 p.u. limit, indicating that the proposed EMS maintains voltage regulation within acceptable operating bounds at

all times. In the GON mode, the voltage variations are more pronounced, with values approximately ranging from 0.04 to 0.09 p.u., reflecting higher system flexibility due to grid interaction. The system utilizes this flexibility to optimize costs, even if it results in greater voltage excursions (still within the limits). In contrast, under GOFF conditions, the voltage regulation is smoother and more stable, approximately ranging from 0.05 to 0.08 p.u., which is consistent with a more conservative control strategy in the absence of grid support.

Finally, Fig. **11** illustrates the maximum line loadability (expressed as a percentage of thermal capacity) across all branches of the 33-node test system for a representative day of operation. The results are shown for both the GON and GOFF modes. The dashed horizontal line at 100 % denotes the maximum allowable thermal limit for each distribution line.

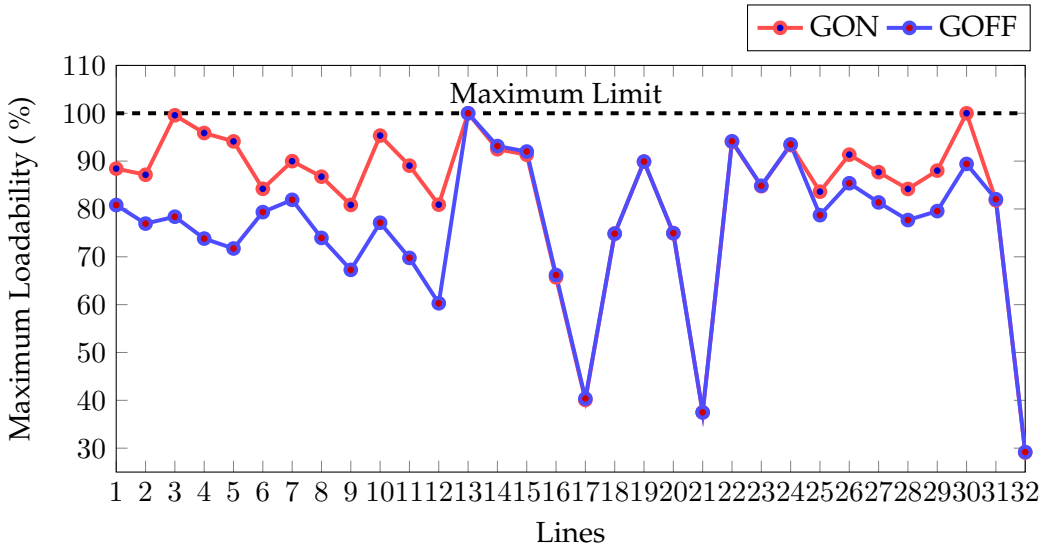

Figure 11. Performance of the maximum loadability in the optimal solution obtained by the PPSO for a representative day of operation

In both modes of operation, the loadability of all lines remains within permissible limits, confirming that the optimization process respects the thermal constraints. Under GON conditions, most lines operate between 85 and 100 % of their capacity, with relatively uniform loading, suggesting that the system leverages the grid connection to balance the power flows efficiently. Under GOFF conditions, greater variability is observed, with several lines operating well below their capacity and others showing reduced load levels (*e.g.*, lines 17, 21, and 32), which is indicative of the redistribution of power flows due to the absence of an external supply.

Figs. **8**, **9**, **10**, and **11** confirm that the PPSO-based EMS ensures full compliance with the SoC, voltage, and current constraints in both modes of operation. The system adapts its charging strategy according to grid availability, operating more flexibly in GON mode and more cautiously in GOFF mode. This highlights the EMS's ability to maintain feasibility, adaptability, and technical soundness in managing BESS operation across different scenarios.

6. Conclusions and future works

This work presented an energy management system for the optimal operation of battery energy storage systems in AC microgrids under grid-connected and islanded modes, using a master-slave strategy that integrates particle swarm optimization with a successive approximations power flow method.

The proposed methodology achieved the lowest operating costs in both GON and GOFF modes when compared to alternative metaheuristics (CBGA and PVSA), the proposed methodology for the GON case also outperformed the exact solution obtained with an SDP model that solves this optimization problem. Specifically, in GON mode, the PPSO-based EMS reached a cost reduction of 101.47 USD/day (1.45 %) relative to the base case, while, in GOFF mode, it achieved a reduction of 23.17 USD/day (0.13 %). PPSO also yielded the lowest average cost, with values of 6900.50 USD/day in GON mode and 17529.72 USD/day in GOFF mode, outperforming the competing methods in both cases. In terms of solution consistency, PPSO exhibited low standard deviations of 0.067 % (GON) and 0.014 % (GOFF) over 100 independent runs. Despite its moderate computational cost (39.16 seconds per run in GON mode 67.91 seconds per run in GOFF mode), the method ensures full compliance with all technical constraints, including SoC limits (10-90 %), voltage regulation (<0.10 p.u.), and line loadability (<100 %), confirming its robustness, feasibility, and effectiveness.

Future work will focus on extending the methodology to formulations that enable the management of both active and reactive power by the BESS, in addition to considering their relocation within the system to further improve operating costs. Likewise, another line of future research may focus on the optimization of technical factors such as network energy losses or environmental factors such as GHG emissions.

7. CRediT author statement

All authors contributed equally to the research.

References

[1] A. Mohammed, S. S. Refaat, S. Bayhan, and H. Abu-Rub, "Ac microgrid control and management strategies: Evaluation and review," *IEEE Power Elect. Mag.*, vol. 6, no. 2, pp. 18–31, 2019. https://doi.org/10.1109/MPEL.2019.2910292 ↑ 4

[2] A. N. Sheta, G. M. Abdulsalam, B. E. Sedhom, and A. A. Eladl, "Comparative framework for ac-microgrid protection schemes: challenges, solutions, real applications, and future trends," *Protect. Control Mod. Power. Syst.*, vol. 8, no. 2, pp. 1–40, 2023. https://doi.org/10.1186/s41601-023-00296-9 ↑ 4

[3] R. Kandari, N. Neeraj, and A. Micallef, "Review on recent strategies for integrating energy storage systems in microgrids," 2023. [Online]. Available: https://doi.org/10.3390/en16010317 ↑ 4

[4] M. Uzair, L. Li, M. Eskandari, J. Hossain, and J. G. Zhu, "Challenges, advances and future trends in ac microgrid protection: With a focus on intelligent learning methods," *Renew. Sust. Energy Rev.*, vol. 178, p. 113228, 2023. https://doi.org/10.1016/j.rser.2023.113228 ↑ 4

[5] A. A. R. Mohamed, R. J. Best, X. Liu, and D. J. Morrow, "Two-phase bess optimization methodology to enhance the distribution network power quality and mitigate violations," *IET Renew. Power Gen.*, vol. 17, no. 11, pp. 2895–2908, 2023. https://doi.org/10.1049/rpg2.12583 ↑ 4

[6] N. I. Labra-Cáceres, L. F. Grisales-Noreña, R. I. Bolaños, J. A. Guzmán-Henao, and O. D. Montoya, "Energy management system for PV-based distributed generators in AC microgrids using an adapted JAYA optimizer to minimize operational costs, energy losses, and CO2 emissions," *Res. Eng.*, p. 104397, 2025. https://doi.org/10.1016/j.rineng.2025.104397 ↑ 5

[7] L. F. Grisales-Noreña, H. P. Vega, O. D. Montoya, V. Botero-Gómez, and D. Sanin-Villa, "Cost optimization of ac microgrids in grid-connected and isolated modes using a population-based genetic algorithm for energy management of distributed wind turbines," *Mathematics*, vol. 13, no. 5, p. 704, 2025. https://doi.org/10.3390/math13050704 ↑ 5

[8] A. Rajagopalan, K. Nagarajan, O. D. Montoya, S. Dhanasekaran, I. A. Kareem, A. S. Perumal, N. Lakshmaiya, and P. Paramasivam, "Multi-objective optimal scheduling of a microgrid using oppositional gradient-based grey wolf optimizer," *Energies*, vol. 15, no. 23, p. 9024, 2022. https://doi.org/10.3390/en15239024 ↑ 5, 8

[9] L. Grisales-Noreña, B. Cortés-Caicedo, O. D. Montoya, J. Hernandéz, and G. Alcalá, "A battery energy management system to improve the financial, technical, and environmental indicators of colombian urban and rural networks," *Journal of Energy Storage*, vol. 65, p. 107199, 2023. https://doi.org/10.1016/j.est.2023.107199 ↑ 5, 8, 12, 15, 18

[10] Q. Yan, Z. Wang, L. Xing, and C. Zhu, "Optimal economic analysis of battery energy storage system integrated with electric vehicles for voltage regulation in photovoltaics connected distribution system," *Sustainability*, vol. 16, no. 19, p. 8497, 2024. https://doi.org/10.3390/su16198497 ↑ 6, 8

[11] S. Alexprabu and K. Sathiyasekar, "Battery energy management systems in active distribution network," in *2023 4th Int. Conf. Smart Elect. Comm. (ICOSEC)*. IEEE, 2023, pp. 194–200. https://10.1109/ICPCSN58827.2023.00123 ↑ 6, 8

[12] Y. Sahri, Y. Belkhier, S. Tamalouzt, N. Ullah, R. N. Shaw, M. S. Chowdhury, and K. Techato, "Energy management system for hybrid pv/wind/battery/fuel cell in microgrid-based hydrogen and economical hybrid battery/super capacitor energy storage," *Energies*, vol. 14, no. 18, p. 5722, 2021. https://doi.org/10.3390/en14185722 ↑ 6, 8

[13] T. A. Fagundes, G. H. F. Fuzato, L. J. R. Silva, A. M. dos Santos Alonso, J. C. Vasquez, J. M. Guerrero, and R. Q. Machado, "Battery energy storage systems in microgrids: A review of soc balancing and perspectives," *IEEE Op. J. Ind Elect. Soc.*, 2024. https://doi.org/10.1109/OJIES.2024.3455239 ↑ 6, 8

[14] S. Wang, Q. Tan, X. Ding, and J. Li, "Efficient microgrid energy management with neural-fuzzy optimization," *Int. J. Hydrogen Energy*, vol. 64, pp. 269–281, 2024. https://doi.org/10.1016/j.ijhydene.2024.03.291 ↑ 7, 8

[15] R. Nebuloni, L. Meraldi, C. Bovo, V. Ilea, A. Berizzi, S. Sinha, R. B. Tamirisakandala, and P. Raboni, "A hierarchical two-level milp optimization model for the management of grid-connected bess considering accurate physical model," *App.Energy*, vol. 334, p. 120697, 2023. https://doi.org/10.1016/j.apenergy.2023.120697 ↑ 7, 8

[16] S. Behera and N. B. Dev Choudhury, "A systematic review of energy management system based on various adaptive controllers with optimization algorithm on a smart microgrid," *Int. Trans. Elect. Energy Syst.*, vol. 31, no. 12, p. e13132, 2021. https://doi.org/10.1002/2050-7038.13132 ↑ 7

[17] A. Kazikova, M. Pluhacek, and R. Senkerik, "Why tuning the control parameters of metaheuristic algorithms is so important for fair comparison?" *Mendel*, vol. 26, no. 2, pp. 9–16, 2020. https://doi.org/10.13164/mendel.2020.2.009 ↑ 7

[18] C. Huang, Y. Li, and X. Yao, "A survey of automatic parameter tuning methods for metaheuristics," *IEEE Trans. Evol. Comp.*, vol. 24, no. 2, pp. 201–216, 2019. https://doi.org/10.1109/TEVC.2019.2921598 ↑ 7

[19] L. S. Avellaneda-Gomez, L. F. Grisales-Noreña, B. Cortés-Caicedo, O. D. Montoya, and R. I. Bolaños, "Optimal battery operation for the optimization of power distribution networks: An application of the ant lion optimizer," *J. Energy Storage*, vol. 84, p. 110684, 2024. https://doi.org/10.1016/j.est.2024.110684 ↑ 9

[20] M. Issa, H. Ibrahim, H. Hosni, A. Ilinca, and M. Rezkallah, "Effects of low charge and environmental conditions on diesel generators operation," *Eng*, vol. 1, no. 2, pp. 137–152, 2020. https://doi.org/10.3390/eng1020009 ↑ 10

[21] A. Soroudi, *Power system optimization modeling in GAMS*. Springer, 2017, vol. 78. https://doi.org/10.1007/978-3-319-62350-4 ↑ 11

[22] F. Marini and B. Walczak, "Particle swarm optimization (pso). a tutorial," *Chemometrics Intell. Lab. Syst.*, vol. 149, pp. 153–165, 2015. https://doi.org/10.1016/j.chemolab.2015.08.020 ↑ 11

[23] S. Charadi, H. E. Chakir, A. Redouane, A. El Hasnaoui, and M. Et-taoussi, "Bi-objective optimal active and reactive power flow management in grid-connected AC/DC hybrid microgrids using metaheuristic–PSO," *Clean Energy*, vol. 7, no. 6, pp. 1356–1380, 12 2023. https://doi.org/10.1093/ce/zkad081 ↑ 11

[24] D. Wang, D. Tan, and L. Liu, "Particle swarm optimization algorithm: an overview," *Soft Comp.*, vol. 22, no. 2, pp. 387–408, 2018. https://doi.org/10.1007/s00500-016-2474-6 ↑ 11

[25] V. Kusuma, A. Firdaus, S. Suprapto, D. Putra, Y. Prasetyo, and F. Filliana, "Leveraging pso algorithms to achieve optimal stand-alone microgrid performance with a focus on battery lifetime," *Int. J. App. Power Eng.*, vol. 12, no. 3, pp. 293–299, Sep. 2023. https://doi.org/10.11591/ijape.v12.i3.pp293-299 ↑ 13, 18

[26] O. D. Montoya and W. Gil-González, "On the numerical analysis based on successive approximations for power flow problems in ac distribution systems," *Elect. Power Syst. Res.*, vol. 187, p. 106454, 2020. https://doi.org/10.1016/j.epsr.2020.106454 ↑ 13

[27] M. E. Baran and A. W. Kelley, "A branch-current-based state estimation method for distribution systems," *IEEE Trans. Power Syst.*, vol. 10, no. 1, pp. 483–491, 1995. https://doi.org/10.1109/59.373974 ↑ 15

[28] A. Hirsch, Y. Parag, and J. Guerrero, "Microgrids: A review of technologies, key drivers, and outstanding issues," *Renew. Sust. Energy Rev.*, vol. 90, 04 2018. 10.1016/j.rser.2018.03.040 ↑ 15

[29] S. Parhizi, A. Khodaei, and S. Bahramirad, "State of the art in research on microgrids: A review," *IEEE Access*, vol. 3, pp. 1–1, 01 2015. 10.1109/ACCESS.2015.2443119 ↑ 15

[30] W. Gil-González, O. D. Montoya, L. F. Grisales-Noreña, and A. Escobar-Mejía, "Optimal economic–environmental operation of bess in ac distribution systems: A convex multi-objective formulation," *Computation*, vol. 9, no. 12, p. 137, 2021. https://doi.org/10.3390/computation9120137 ↑ 16

[31] *Tensiones y Frecuencia Nominales en Sistemas de Energa Eléctrica En Redes de Servicio Público NTC 1340*, I.C. de Normas Técnicas y Certificación (ICONTEC), 2004. ↑ 16

[32] B. Cortés-Caicedo, L. F. Grisales-Noreña, O. D. Montoya, M. A. Rodriguez-Cabal, and J. A. Rosero, "Energy management system for the optimal operation of pv generators in distribution systems using the antlion optimizer: A colombian urban and rural case study," *Sustainability*, vol. 14, no. 23, p. 16083, 2022. https://doi.org/10.3390/su142316083 ↑ 17

[33] B. Doğan and T. Ölmez, "A new metaheuristic for numerical function optimization: Vortex search algorithm," *Info. Sci.*, vol. 293, pp. 125–145, 2015. https://doi.org/10.1016/j.ins.2014.08.053 ↑ 18

[34] P. C. Chu and J. E. Beasley, "A genetic algorithm for the multidimensional knapsack problem," *J. Heuristics*, vol. 4, pp. 63–86, 1998. ↑ 18

[35] R. W. Hockney and C. R. Jesshope, *Parallel Computers 2: architecture, programming and algorithms*. CRC Press, 2019. https://doi.org/10.1201/9780367810672 ↑ 19

[36] D.-H. Yoon and Y. Han, "Parallel power flow computation trends and applications: A review focusing on gpu," *Energies*, vol. 13, no. 9, p. 2147, 2020. https://doi.org/10.3390/en13092147 ↑ 19

[37] S. Lalwani, H. Sharma, S. C. Satapathy, K. Deep, and J. C. Bansal, "A survey on parallel particle swarm optimization algorithms," *Arabian J. Sci. Eng.*, vol. 44, pp. 2899–2923, 2019. https://doi.org/10.1007/s13369-018-03713-6 ↑ 19

[38] L. F. Grisales-Noreña, O. D. Montoya, E.-J. Marín-García, C. A. Ramos-Paja, and A.-J. Perea-Moreno, "Integration of pv distributed generators into electrical networks for investment and energy purchase costs reduction by using a discrete–continuous parallel pso," *Energies*, vol. 15, no. 20, p. 7465, 2022. https://doi.org/10.3390/en15207465 ↑ 19

[39] P. Chu and J. Beasley, *A genetic algorithm for the set partitioning problem*. London, UK: Imperial College, 1995. ↑ 19

[40] V. M. Garrido-Arévalo, O. D. Montoya, W. Gil-González, L. F. Grisales-Noreña, and J. C. Hernández, "An sdp relaxation in the complex domain for the efficient coordination of bess and dgs in single-phase distribution grids while considering reactive power capabilities," *J. Energy Storage*, vol. 90, p. 111913, 2024. https://doi.org/10.1016/j.est.2024.111913 ↑ 20

Hugo Alessandro Figueroa-Saavedra

Born in Talca, Chile, in 1996, he earned his degree in Electrical Civil Engineering from the Universidad de Talca in 2023, with a Minor in Industrial Electronics. Since 2024, he has been pursuing a MSc in Engineering and Energy Conversion at Universidad de Talca, and, in 2025, he also began his PhD in Electrical Engineering Sciences at the same university. He has co-instructed the elective course titled *Metaheuristic Optimization for Electrical Systems* and served as a teaching assistant in various subjects. He is a member of the Power Systems Operation and Planning Laboratory (LOPSE) and, since 2024, he has held the positions of Secretary and WebMaster for the IEEE Student Branch. His research interests include mathematical optimization, power systems planning and control, renewable energy, and energy storage.

Email: hfigueroa14@alumnos.utalca.cl

Luis Fernando Grisales Noreña

A senior Minciencias researcher, he was born in Cartago, Valle, Colombia, in 1990. He is an electrical engineer and holds a Master's degree in Electrical Engineering from Universidad Tecnológica de Pereira. He earned a PhD in Automatic Engineering from Universidad Nacional de Colombia and a PhD in Renewable Energies from the University of Jaén. His academic and professional work has focused on the study of electrical networks, the development of energy management strategies, and the modeling and optimization of power systems. He has led various research projects and has published extensively in the field of intelligent power systems operation. He is currently affiliated with Universidad del Valle as an Assistant Professor and is part of the GRALTA Research Group.

Email: grisales.luis@correounivalle.edu.co

Brandon Cortés Caicedo

A junior Minciencias researcher, he was born in Bogotá, Colombia, in 1999. He holds a degree in Electrical Engineering from Universidad Distrital Francisco José de Caldas and a Master's degree in Industrial Energy Management from Instituto Tecnológico Metropolitano de Medellín. He is currently a PhD student in Engineering at Universidad Distrital Francisco José de Caldas. He serves as a full-time professor at Institución Universitaria Pascual Bravo in Medellín. He is a member of the Environmental Research and Innovation Group (GIAM) of Institución Universitaria Pascual Bravo, as well as of the Compatibility and Electromagnetic Interference Group (GCEM) of Universidad Distrital Francisco José de Caldas. His research interests focus on optimization applied to the planning and operation of electrical distribution systems.

Email: brandon.cortes@pascualbravo.edu.co